

## Freed-Isobar Analysis of Light Mesons at COMPASS

F. Krinner\* for the COMPASS collaboration

*Max Planck Institut for Physics,  
80805 Munich, Bavaria, Germany*

*\*E-mail: fkrinner@mpp.mpg.de*

Modern hadron-spectroscopy experiments such as COMPASS collect data samples of unprecedented size, so that novel analysis techniques become possible and necessary. One such technique is the freed-isobar partial-wave analysis (PWA). In this approach, fixed parametrizations for the amplitudes of intermediate states commonly modeled using Breit-Wigner shapes are replaced by sets of step-like functions that are determined from the data. This approach not only reduces the model dependence of partial-wave analyses, but also allows us to study the amplitudes of the intermediate states and their dependence on the parent system.

We will also present results of a freed-isobar PWA performed on the large data set on diffractive production of three charged pions collected by the COMPASS experiment, which consists of  $46 \times 10^6$  exclusive events. We will focus on results for the wave with spin-exotic quantum numbers  $J^{PC} = 1^{-+}$ , in particular on its decay into  $\rho(770)\pi$ . Here, the freed-isobar PWA method provides insight into the interplay of three- and two-particle dynamics and confirms the decay of the spin-exotic  $\pi_1(1600)$  resonance to  $\rho(770)\pi$  in a model-independent way.

*Keywords:* Exotic; model independent; partial-wave analysis; PWA; freed-isobar.

### 1. Diffractive $3\pi$ production

The data set presented here was collected in 2008 by the COMPASS experiment located at CERN's North Area using a  $190 \text{ GeV}/c \pi^-$  beam impinging on liquid hydrogen serving as a proton target. Using the two-stage COMPASS spectrometer, the process

$$\pi_{\text{beam}}^- + p_{\text{target}} \rightarrow \pi^- \pi^+ \pi^- + p_{\text{recoil}} \quad (1)$$

is selected resulting in a sample of  $46 \times 10^6$  exclusive events. These events have been analyzed in an extensive PWA<sup>1</sup> and the resonance parameters of eleven isovector  $3\pi$  resonances have been extracted<sup>2</sup>.

## 2. Freed-isobar PWA method

The measured intensity distribution  $\mathcal{I}(\vec{\tau})$  for a given  $m_{3\pi}$  and  $t'$  bin is a function of the five phase space variables  $\vec{\tau}$  and is modeled as the modulus square of a coherent sum over partial-wave amplitudes:

$$\mathcal{I}(\vec{\tau}) = \left| \sum_{\text{waves}} \mathcal{T}_{\text{wave}} \mathcal{A}_{\text{wave}}(\vec{\tau}) \right|^2. \quad (2)$$

Here, the complex-valued transition amplitudes  $\mathcal{T}_{\text{wave}}$  encode the strengths and phases with which single partial waves contribute and the decay amplitudes  $\mathcal{A}_{\text{wave}}(\vec{\tau})$  describe the  $3\pi$  decay and encode the  $\vec{\tau}$ -dependence of the partial waves.

The conventional PWA model uses a set of 88 partial waves that differ in spin quantum numbers and  $2\pi$  resonance content<sup>1</sup>. The decay amplitudes are split up under the assumption that production and decay of appearing  $2\pi$  and  $3\pi$  resonances factorize and the process can therefore be described as two subsequent two-particle decays. This assumption is known as the isobar model:

$$\mathcal{A}_{\text{wave}}(\vec{\tau}) = \psi_{\text{wave}}(\vec{\tau}) \Delta_{\text{wave}}(m_{\pi\pi}) + \text{Bose symm.}, \quad (3)$$

where  $\psi_{\text{wave}}(\vec{\tau})$  describes the dependence of the partial wave on the decay angles which is fully determined from first principles by the appearing spin quantum numbers. The dynamic isobar amplitudes  $\Delta_{\text{wave}}(m_{\pi\pi})$  in contrast describe the  $2\pi$  resonance content—or isobar—of the partial waves and have to be known beforehand. Bose symmetrization is necessary due to the two identical final-state  $\pi^-$ .

The choice of  $2\pi$  resonance content, its parameterizations and its parameters introduces possible model bias to the partial wave model and neglects possible contributions from low-intensity resonances or final-state interactions of the isobar with the third pion. To overcome this, we re-analyzed the data set using the freed-isobar approach, in which we replace the fixed dynamic isobar amplitudes by sets of indicator functions spanning the kinematically allowed  $m_{\pi\pi}$  range:

$$\Delta_{\text{wave}}(m_{\pi\pi}) \rightarrow \sum_{\text{bins}} \Delta_{\text{wave}}^{\text{bin}}(m_{\pi\pi}) \quad \text{with} \quad \Delta_{\text{wave}}^{\text{bin}}(m_{\pi\pi}) = \begin{cases} 1 & m_{\pi\pi} \in \text{bin}, \\ 0 & \text{otherwise.} \end{cases} \quad (4)$$

This replacement alleviates the necessity for fixed dynamic isobar amplitudes from the partial wave model, resulting in a much higher number of

parameters, that can lead to mathematical ambiguities within the model—so-called zero modes—that have to be identified and resolved. The detailed origin of these ambiguities in general and for the data presented here is discussed in Refs. [3–5].

We replaced the dynamic isobar parameterizations of 12 of the 88 waves in the PWA model of Ref. [1] following eq. 4. Eleven of these waves represent the waves describing the largest intensities in the model, so that 75% of the total intensity is described by the freed waves. This minimizes possible effects of imperfections in the fixed isobar parameterizations of the remaining waves. The twelfth wave is the spin-exotic  $1^{-+}1^{+}[\pi\pi]_{1--}\pi\text{P}$  wave<sup>a</sup>, which will be presented in Sec. 3. We use an  $m_{\pi\pi}$  bin width of  $40\text{ MeV}/c^2$ , and a region of narrower bins of  $20\text{ MeV}/c^2$  around the  $\rho(770)$  resonance. The analysis was performed in 50 equidistant bins in the mass range  $0.5 < m_{3\pi} < 2.5\text{ GeV}/c^2$  and four non-equidistant bins in the squared four-momentum transfer  $t'$ , resulting in 200 independently fitted kinematic cells.

### 3. Results for the spin-exotic wave

The result of this analysis is shown in Fig. 2. As expected, the resulting two-dimensional intensity distribution on the right side is dominated by a clear peak corresponding to the decay  $\pi_1(1600) \rightarrow \rho(770)\pi$ . This confirms the existence of this decay without any assumption on the dynamic amplitude of the  $[\pi\pi]_{1--}$  system. The left plot shows the coherent sum of all  $m_{\pi\pi}$  bins, compared to the result from the conventional PWA. Both distributions are dominated by a similar peak corresponding to the  $\pi_1(1600)$  resonance. The freed-isobar result has a higher over-all intensity, since it also can pick up intensity away from the  $\rho(770)$  peak.

Fig. 1 shows the results of the analysis of the data in the highest  $t'$  bin for three  $m_{3\pi}$  bins, below, on, and above the nominal mass of the  $\pi_1(1600)$  resonance. The left column shows the resulting intensity distributions and the right column shows the same data as Argand diagrams. In all three  $m_{3\pi}$  bins, the fixed Breit-Wigner amplitude from the conventional PWA agrees nicely with the result of the freed-isobar analysis.

The intensity distribution assumes its highest value in the  $m_{3\pi}$  at the  $\pi_1(1600)$  mass and the Argand diagrams rotate counter-clockwise moving

<sup>a</sup>The wave name is given by  $J_{3\pi}^{PC} M^{\epsilon} [\pi\pi]_{J_{\pi\pi}^{PC}} \pi L$ , where  $J^{PC}$  are the quantum number of the  $3\pi$  and  $\pi\pi$  systems,  $M^{\epsilon}$  is the spin-projection and reflectivity quantum number of the  $3\pi$  system and  $L$  is the orbital angular between the  $\pi\pi$  system and the third pion.

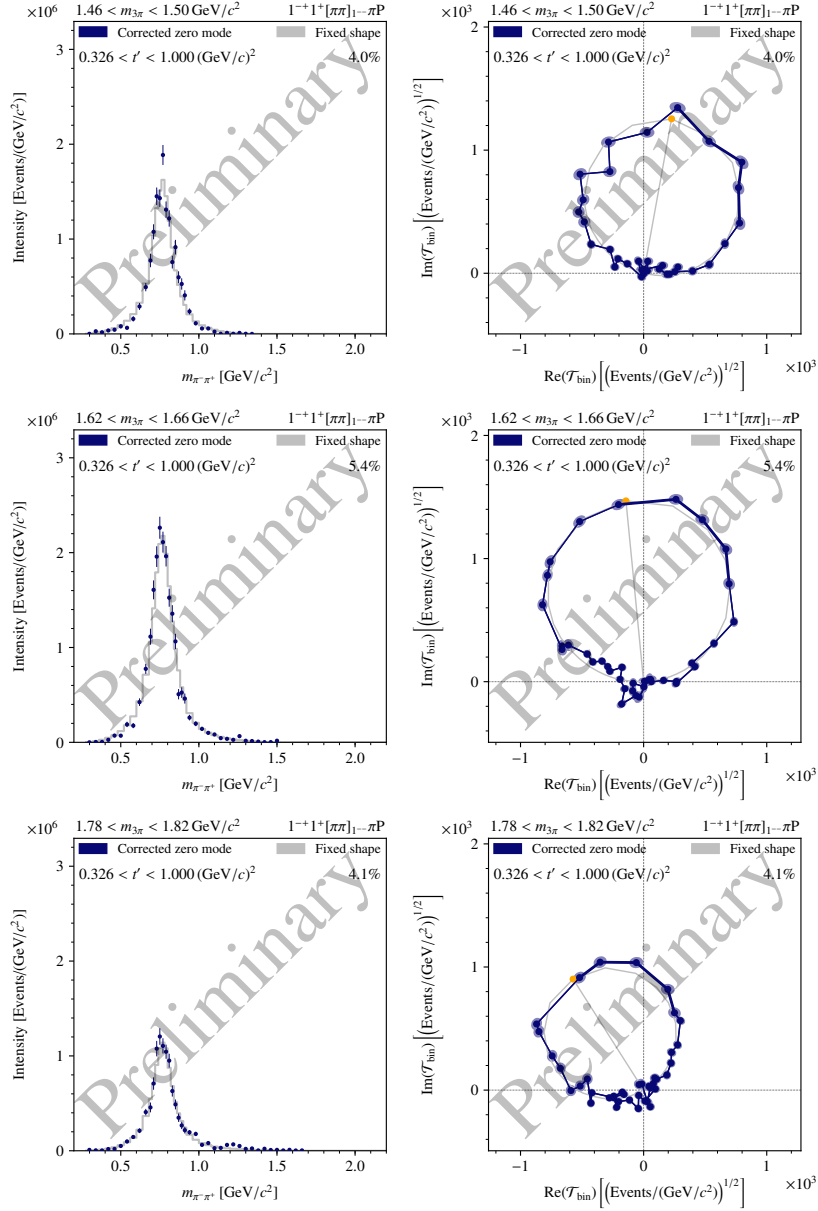


Fig. 1. Results of the freed-isobar PWA for three  $m_{3\pi}$  bins (rows) in the highest  $t'$  bin for the  $1^{-+}1^{+}[\pi\pi]_{1--}\pi P$  wave (blue). The Breit-Wigner amplitude for the  $\rho(770)$  as used in the conventional PWA is overlaid in gray. Left: Intensity distributions. Right: Argand diagrams; the orange dot indicates the nominal resonance position of the gray curve.

through the  $\pi_1(1600)$  resonance, which both reflects the dynamic amplitude of the  $\pi_1(1600)$  mother resonance, which further confirms its existence.

Since the fixed Breit-Wigner amplitude is adequate for all  $m_{3\pi}$  slices in Fig. 1, we show two additional bins in Fig. 3 where the shapes do not match equally well. At low  $m_{3\pi}$  the dynamic isobar amplitude, exhibits a sharper peak than the fixed Breit-Wigner, i.e. a slightly deformed Argand circle. At high  $m_{3\pi}$ , it exhibits a second peak in the intensity spectrum at a two-pion mass of  $1.6 \text{ GeV}/c^2$ , which could correspond to an excited  $\rho'$  and is unaccounted for in the conventional approach. Whether this peak actually stems from a resonance, requires a subsequent resonance-model fit.

#### 4. Conclusion

We showed results for the dynamic isobar amplitudes of the spin-exotic  $1^{-+}1^{+}[\pi\pi]_{1--}\pi\text{P}$  wave extracted from COMPASS data on diffractively produced  $3\pi$  using the freed-isobar approach<sup>3-5</sup>. The extracted dynamic isobar amplitudes are in general in agreement with the assumption of a dominant presence of the  $\rho(770)$  resonance in the  $\pi\pi$  P-wave wave as assumed in the conventional PWA approach<sup>1</sup>. In addition, the  $\pi_1(1600)$  is confirmed to appear in this partial wave. Nevertheless, there are deviations from the Breit-Wigner amplitude that may originate from distortions of the dynamic isobar amplitude due to non-resonant contributions, such as the Deck effect<sup>6</sup> or re-scattering effects, or additional excited isobar resonances. To clarify the origin of these deviations, a resonance-model fit to the presented data is work in progress.

#### References

1. C. Adolph *et al.*, Resonance Production and  $\pi\pi$  S-wave in  $\pi^{-}+p \rightarrow \pi^{-}\pi^{-}\pi^{+}+p_{\text{recoil}}$  at  $190 \text{ GeV}/c$ , *Phys. Rev.* **D95**, p. 032004 (2017).
2. M. Aghasyan *et al.*, Light isovector resonances in  $\pi^{-}p \rightarrow \pi^{-}\pi^{-}\pi^{+}p$  at  $190 \text{ GeV}/c$ , *Phys. Rev.* **D98**, p. 092003 (2018).
3. F. Krinner, D. Greenwald, D. Ryabchikov, B. Grube and S. Paul, Ambiguities in model-independent partial-wave analysis, *Phys. Rev.* **D97**, p. 114008 (2018).
4. F. Krinner, Recent progress in the partial-wave analysis of the diffractively produced  $\pi^{-}\pi^{+}\pi^{-}$  final state at COMPASS, *EPJ Web Conf.* **199**, p. 02003 (2019).
5. F. Krinner, Freed-Isobar Partial-Wave Analysis, PhD thesis, Technische Universität München (2018).
6. R. T. Deck, Kinematical interpretation of the first  $\pi-\rho$  resonance, *Phys. Rev. Lett.* **13**, p. 169 (1964).

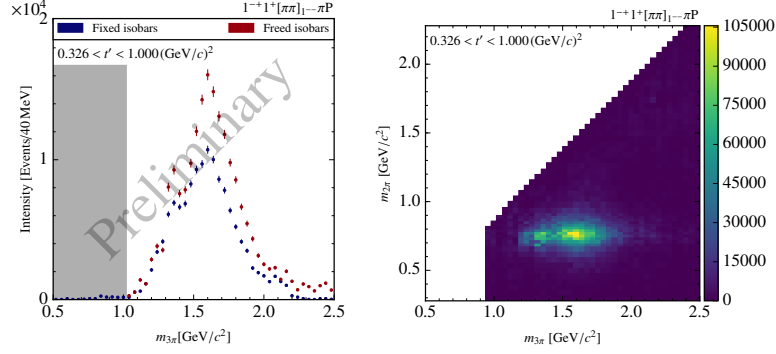


Fig. 2. Results of the freed-isobar analysis for the  $1^{-+}1^{+}[\pi\pi]_{1--}\pi P$  wave in the highest  $t'$  bin. Left: coherent sum over all  $m_{\pi\pi}$  bins (red) compared to the corresponding result of the conventional PWA (blue). Right: Two-dimensional intensity distribution as function of  $m_{3\pi}$  and  $m_{\pi\pi}$ .

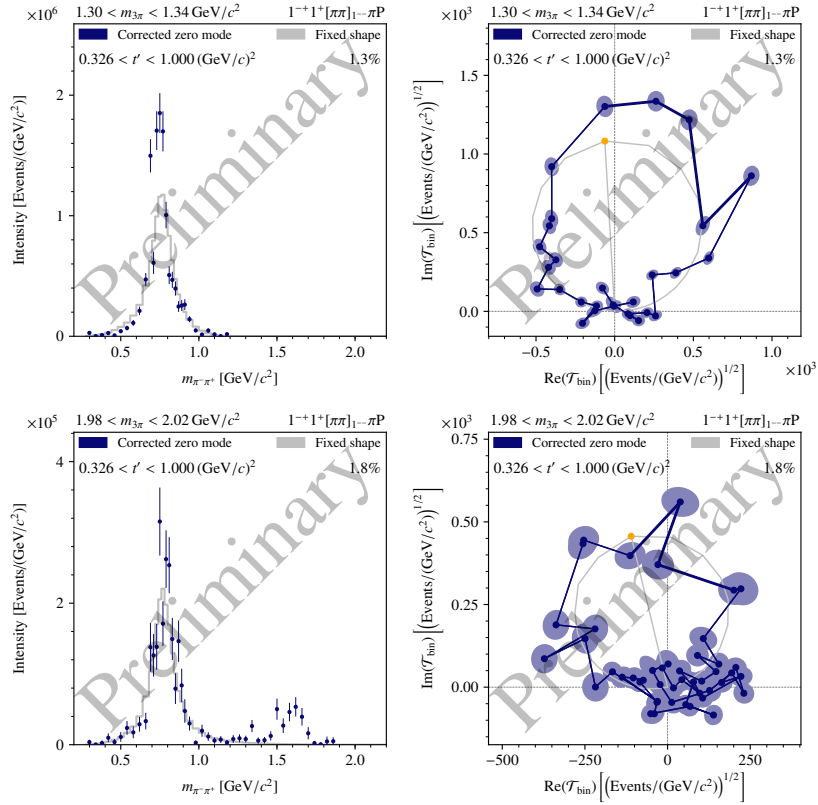


Fig. 3. As Fig. 1 for two additional  $m_{3\pi}$  bins far away from the  $\pi_1(1600)$  region.